JACS
JOURNAL OF THE AMERICAN CHEMICAL SOCIETY
pubs.acs.org/JACS
Article

Role of Anions and Mixtures of Anions on the Thermochromism, Vapochromism, and Polymorph Formation of Luminescent Crystals of a Single Cation, $[(C_6H_{11}NC)_2Au]^+$

Lucy M. C. Luong, Mark A. Malwitz, Venoos Moshayedi, Marilyn M. Olmstead, and Alan L. Balch*

Cite This: J. Am. Chem. Soc. 2020, 142, 5689−5701
Read Online

ABSTRACT: Noncoordinating anions, which generally play a subordinate role in coordination chemistry, alter the structure, the luminescence, as well as the thermochromic and vapochromic behaviors of salts of the two-coordinate cation, $[(C_6H_{11}NC)_2Au]^+$. Thus whereas the yellow polymorphs of $[(C_6H_{11}NC)_2Au](PF_6)$ and $[(C_6H_{11}NC)_2Au](AsF_6)$ contain single chains of cations and are vapochromic, yellow $[(C_6H_{11}NC)_2Au](SbF_6)$ does not form the same polymorph and is not vapochromic but contains two distinct chains of cations connected through aurophilic interactions. Mixed crystals such as $[(C_6H_{11}NC)_2Au](PF_6)_{0.50}(AsF_6)_{0.50}$ have been prepared by adding diethyl ether to a dichloromethane solution containing equimolar amounts of $[(C_6H_{11}NC)_2Au](PF_6)$ and $[(C_6H_{11}NC)_2Au](AsF_6)$. The initial (kinetic) product for the three combinations of anions $((PF_6)^-/(AsF_6)^-$, $(PF_6)^-/(SbF_6)^-$, and $(AsF_6)^-/(SbF_6)^-)$ was a precipitate of fine yellow needles with a green emission, which were gradually transformed at rates that depended on the anions present into colorless crystals with a blue emission. Whereas neither polymorph of $[(C_6H_{11}NC)_2Au](PF_6)$ nor $[(C_6H_{11}NC)_2Au](SbF_6)$ is thermochromic, the colorless mixed crystal $[(C_6H_{11}NC)_2Au](PF_6)_{0.50}(SbF_6)_{0.50}$ is thermochromic and converts from blue-emitting to green-emitting at 87−95 °C. The temperature required to transform a crystal of the type $[(C_6H_{11}NC)_2Au](PF_6)_n(AsF_6)_{1-n}$ from colorless (blue-emitting) to yellow (green-emitting) increases as the fraction of hexafluorophosphate ion in the crystal increases. The yellow crystals of $[(C_6H_{11}NC)_2Au](PF_6)_{0.75}(AsF_6)_{0.25}$, $[(C_6H_{11}NC)_2Au](PF_6)_{0.50}(AsF_6)_{0.50}$, and $[(C_6H_{11}NC)_2Au](PF_6)_{0.25}(AsF_6)_{0.75}$ are vapochromic, whereas the yellow crystals of $[(C_6H_{11}NC)_2Au](PF_6)_{0.50}(SbF_6)_{0.50}$ and $[(C_6H_{11}NC)_2Au](AsF_6)_{0.50}(SbF_6)_{0.50}$ are not.

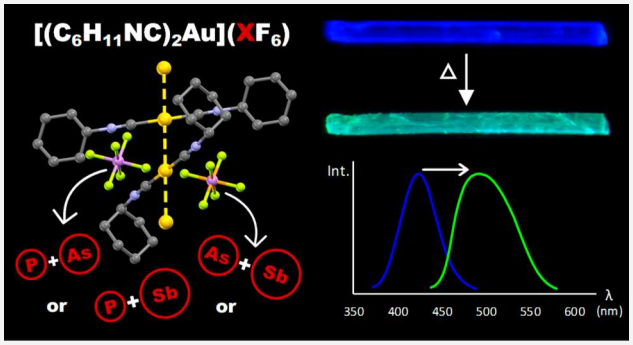

INTRODUCTION

Crystals are widely admired for their transparency (e.g., the phrase, "crystal clear"), color, shiny angular surfaces, and stability. The stable, ordered array of ions or molecules inside provides an environment that allows definitive structural analysis by X-ray diffraction. Consequently, it is somewhat surprising that some crystals have a dynamic nature and can undergo transformations in their color and luminescence in response to external stimuli such as heat,[1−3] pressure,[4−7] light,[8] or the presence of various vapors.[9,10] Such transformations are particularly easy to observe visually and may be reversible or irreversible. Crystals that are responsive to various environmental factors are useful as sensors, labels for biomaterials, thermal coatings for windows, and optoelectronic devices.[11,12]

In some cases, crystals display color changes that result from the uptake or loss of guest molecules. For example, double salts of the type $[Pt(CNAr)_4][Pt(CN)_4]$ display reversible, vapor-induced color changes that involve the absorption of methanol, water, trifluoroethanol, or chloroform. These absorbed molecules form hydrogen bonds to the cyano ligands and cause changes in the extended ···Pt···Pt···Pt··· interactions that run through the crystals.[13−16] Similarly, the metal chain complex $\{Tl[Au(C_6Cl_5)_2]\}_n$ is vapochromic and thermochromic due to the coordination and release (upon heating) of volatile Lewis bases to the thallium ions and corresponding changes in the Tl−Au bonding.[17,18] Crystals of the colorless, four-coordinate pincer complex $HOC_6H_2(CH_2NMe_2)_2PtCl$ turn orange in the presence of sulfur dioxide due to the attachment of sulfur dioxide to the platinum center in a reversible process.[19]

However, there are some crystals that respond to external stimuli without the uptake of other molecules. In particular, transformations between crystalline polymorphs can involve changes in color or luminescence. In crystalline polymorphs, the molecular or ionic contents of the various forms are

Received: December 6, 2019
Published: February 28, 2020

https://dx.doi.org/10.1021/jacs.9b13168
J. Am. Chem. Soc. 2020, 142, 5689−5701

identical, but the ways in which the molecules or ions are arranged differ.[20]

Complexes of gold(I) frequently form luminescent crystals, some of which are sensitive to external stimuli. Two-coordinate gold(I) complexes are prone to self-association that involves aurophilic interactions between neighboring complexes.[21,22] Aurophillic interactions occur from a combination of dispersion and relativistic effects and result in close contacts between the gold(I) centers.[23,24] These aurophilic interactions can vary in different polymorphs and seem to be particularly responsive to changes in the crystal environment. For example, the colorless, red-emitting salt, $[\mu_3\text{-}S(AuCNC_7H_{13})_3](SbF_6)$, crystallizes so that dimers of the cations form and allow close contact between the six gold centers in each dimer.[25] On cooling to 90 K, crystals of $[\mu_3\text{-}S(AuCNC_7H_{13})_3](SbF_6)$ undergo a crystallographic phase change at ca. 150 K that produces two distinct dimers, one with closer Au···Au contacts between the monomeric units and another with longer Au···Au contacts between monomers. The luminescence also changes so that at 90 K, two emission maxima are found at 490 and 680 nm, whereas at room temperature, a single emission is observed at 667 nm.

The cyclic trinuclear complex, tris[μ_2-(1-ethylimidazolato-N3,C2)-gold(I)], shows a reversible change in luminescence from 440 nm at 100 K to 690 nm at 298 K, which has been attributed to an excited-state phase change that is not accompanied by a crystallographic phase change but by an elongation of the aurophilic interactions between trimers, as detected by X-ray diffraction.[26] In another example, the remarkable two-coordinate complex phenyl(phenyl isocyanide)gold(I) crystallizes in two forms: a blue-emitting form with a long Au···Au interaction (5.733 Å) and a yellow-emitting form with a much closer Au···Au contact (3.177 Å).[27,28] The blue-emitting form is readily transformed into the yellow-emitting form by mechanical pressure or by seeding with a crystal of the yellow-emitting form. Once the process is initiated, the blue-emitting form is eventually completely converted into the yellow-emitting form. In a final example, the salt [(1,3-dimethylimidazo[4,5-*b*]pyrazin-2-ylidene)$_2$Au][Au(CN)$_2$] forms cyan- and green-emitting crystals.[29] Grinding the green-emitting form produces the cyan-emitting form, which is further transformed into an amorphous, red-orange-emitting form.

The two-coordinate gold salts $[(C_6H_{11}NC)_2Au](PF_6)$ and $[(C_6H_{11}NC)_2Au](AsF_6)$ crystallize as colorless, blue-emitting crystals or as yellow, green-emitting crystals.[30,31] The colorless crystals are isostructural, whereas the yellow crystals of the two salts are not isostructural. Figure 1 shows the nature of the extended chains of cations that are connected by aurophillic interactions and run through these crystals. The two types of yellow crystals are vapochromic and are converted into the colorless polymorph upon exposure to the vapors of certain organic liquids including dichloromethane, chloroform, ethanol, and methanol. These transformations occur without the uptake of any vapor. Additionally, the colorless polymorph of $[(C_6H_{11}NC)_2Au](AsF_6)$ is thermochromic and transforms into the yellow polymorph upon heating to 98−102 °C without melting. However, the colorless and yellow polymorphs of $[(C_6H_{11}NC)_2Au](PF_6)$ are not thermochromic, nor is the pale-yellow crystal of $[(C_6H_{11}NC)_2Au](SbF_6)$.

Here we examine the crystallization of the cation, $[(C_6H_{11}NC)_2Au]^+$, with the hexafluoroantimonate counterion and the formation of mixed crystals containing two different

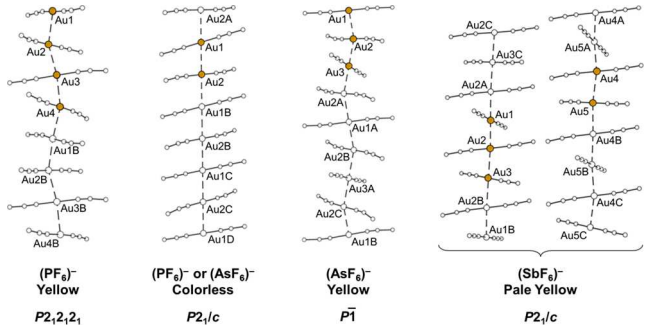

Figure 1. Comparison of the columnar structures of the five different crystalline forms of $[(C_6H_{11}NC)_2Au](EF_6)$ with E = P (ref 30), As (ref 31), or Sb. For clarity, the atoms are represented by arbitrarily sized circles, and only the gold ions and the CNC portion of the ligands attached to the metal are indicated. Aurophilic interactions are shown as dashed lines. Anions are not shown. There are no solvate molecules in any of these crystals.

anions. Noncoordinating anions such as hexafluorophosphate, hexafluoroarsenate, and hexafluoroantimonate generally play a subordinate role in coordination chemistry, where they exhibit minimal interactions with metal centers.[32,33] However, in salts of $[(C_6H_{11}NC)_2Au]^+$, these noncoordinating anions can markedly alter the structures and properties of the crystals that they form. Other cases where anions influence the structures and luminescence of gold(I) complexes are known.[34−37]

RESULTS

Formation and Properties of $[(C_6H_{11}NC)_2Au](SbF_6)$. The salt $[(C_6H_{11}NC)_2Au](SbF_6)$ was prepared by combining chloro(tetrahydrothiophene)gold(I), cyclohexyl isocyanide, and sodium hexafluoroantimonate in acetonitrile. After evaporation of the mixture to dryness, the resulting oil was converted to a yellow powder by dissolution in dichloromethane followed by the addition of diethyl ether. Pale-yellow, blue-luminescent crystals were obtained by the diffusion of diethyl ether into a dichloromethane solution of the yellow powder. No polymorphic form of this salt has been found during extensive studies of it. Like other salts of $[(C_6H_{11}NC)_2Au]^+$, $[(C_6H_{11}NC)_2Au](SbF_6)$ is luminescent.

Figure 2 shows photographs of the emission from crystals of $[(C_6H_{11}NC)_2Au](SbF_6)$ and of the polymorphs of $[(C_6H_{11}NC)_2Au](PF_6)$ and $[(C_6H_{11}NC)_2Au](AsF_6)$ along with the emission and excitation spectra of crystals of $[(C_6H_{11}NC)_2Au](SbF_6)$. Although all of these salts contain a common cation, which is responsible for the emission, each salt shows distinctive luminescence that responds to the differences in aurophilic interactions between the cations in the crystals. However, in dichloromethane solution, $[(C_6H_{11}NC)_2Au](SbF_6)$ is nonluminescent and colorless with absorption features in the UV region: λ_{max}, nm (ε): 216 (9400), 238 (3100), 244 (3400). These values are nearly identical to those of $[(C_6H_{11}NC)_2Au](PF_6)$[30] and $[(C_6H_{11}NC)_2Au](AsF_6)$[31] and are consistent with the presence of monomeric cations in solution. The infrared spectrum of the crystals exhibits isocyanide stretching vibrations at 2934, 2866, and 2846 cm^{-1} and a Sb−F vibration at 651 cm^{-1}.

The pale-yellow, blue-luminescent crystals melted over the temperature range 113−115 °C. No color changes occurred

https://dx.doi.org/10.1021/jacs.9b13168
J. Am. Chem. Soc. 2020, 142, 5689−5701

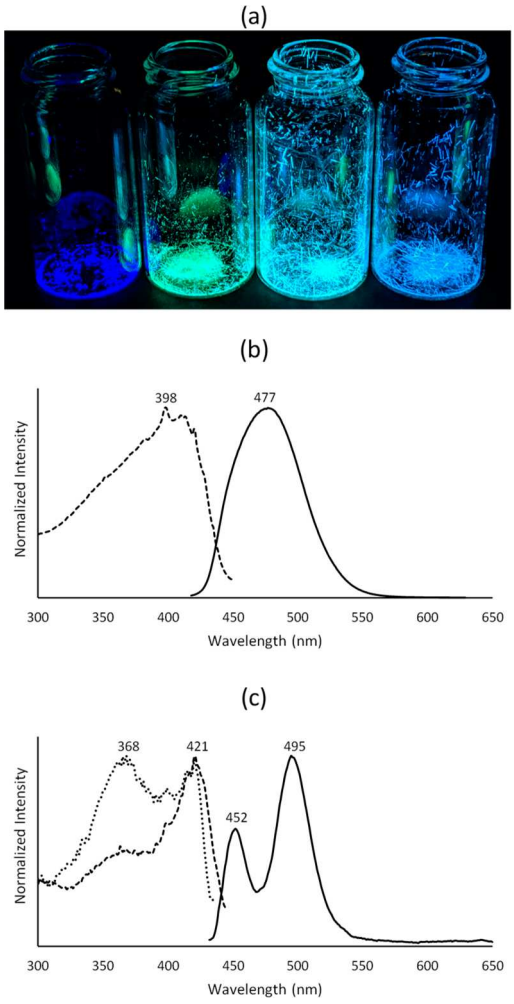

Figure 2. (a) Photographs taken under UV irradiation of crystals from left to right: the colorless polymorph of $[(C_6H_{11}NC)_2Au](PF_6)$, yellow polymorph of $[(C_6H_{11}NC)_2Au](PF_6)$, yellow polymorph of $[(C_6H_{11}NC)_2Au](AsF_6)$, and pale-yellow $[(C_6H_{11}NC)_2Au](SbF_6)$. (b) Excitation spectrum (dashed) for emission at 478 nm and emission spectrum (solid) with excitation at 398 nm of $[(C_6H_{11}NC)_2Au](SbF_6)$ at 298 K. (c) Excitation spectrum (dashed) for emission at 495 nm, excitation spectrum (dotted) for emission at 455 nm, and emission spectrum (solid) with excitation at 390 nm of $[(C_6H_{11}NC)_2Au](SbF_6)$ at 77 K. At 298 K, the emission lifetime is 7.3 μs.

before melting. The melt appeared colorless and was still blue-luminescent. When solidified, the pale-yellow color returned, and blue luminescence was still present.

Vapor experiments were attempted to see if any vapochromic properties were present. No color or luminescence changes were found with exposure of the crystals to acetone, dichloromethane, methanol, acetonitrile, benzene, pyridine, chloroform, toluene, diethyl ether, water, hexane, or pentane vapor.

Crystal Structure of $[(C_6H_{11}NC)_2Au](SbF_6)$. The crystallographic data given in Table 1 indicate that $[(C_6H_{11}NC)_2Au](SbF_6)$ crystallizes in a form that is entirely different from any of the colorless or yellow polymorphs of $[(C_6H_{11}NC)_2Au](PF_6)$ and $[(C_6H_{11}NC)_2Au](AsF_6)$. (See Figure 1.) A portion of the structure of $[(C_6H_{11}NC)_2Au](SbF_6)$ is shown in Figure 3. The crystal contains two different chains of cations that both run parallel to the crystallographic *c* axis. Within one chain, Au1 and Au3 reside on centers of symmetry, whereas Au2 is in a general position. In the other chain, Au4 and Au5 reside in general positions. In the chains, aurophilic interactions connect the gold ions, which are coordinated to two isocyanide ligands in a linear fashion. The distances between the gold atoms are Au1−Au2, 3.0252(7) Å, and Au2−Au3, 3.0858(7) Å, in one chain, and Au4−Au5, 3.0424(9) Å, and Au4−Au5A, 3.0782(9) Å, in the other chain. The closest Au/F contacts are 2.103 for Au3 in one chain and 3.127 for Au5 in the other chain. There are numerous close C−H···F−P contacts between the cyclohexyl rings and the anions.

Along each of the two chains, the cyclohexyl groups alternate between axial orientations in one cation and equatorial positions in the next cation. This alternation between the axial and equatorial disposition of the cyclohexyl groups along the chains of cations is a common feature in the structures in all crystals of $[(C_6H_{11}NC)_2Au](EF_6)$ with E = P, As, or Sb. The anions are positioned between the chains of cations and show no interaction with the gold(I) ions.

Formation of Yellow, Green-Luminescent and Colorless, Blue-Emitting Crystals with Mixed Anions. Yellow and colorless crystals were obtained sequentially by mixing dichloromethane solutions of one salt of $[(C_6H_{11}NC)_2Au]^+$ with a solution of a different salt of $[(C_6H_{11}NC)_2Au]^+$ followed by the addition of diethyl ether. The procedure for the growth of crystals of $[(C_6H_{11}NC)_2Au](PF_6)_{0.50}(AsF_6)_{0.50}$ is set out in Figure 4. Initially, a dichloromethane solution containing equimolar amounts of $[(C_6H_{11}NC)_2Au](PF_6)$ and $[(C_6H_{11}NC)_2Au](AsF_6)$ was prepared and placed in a vial, as shown in part 1 of the figure. Subsequently, diethyl ether was carefully layered over the dichloromethane solution with minimal mixing. As the two solutions diffused together, fine yellow crystals with a green emission formed. To facilitate the removal of these crystals, much of the mother liquor was removed by the use of a pipet. However, these yellow crystals proved to be too small for single-crystal X-ray diffraction. The yellow crystals were stored in contact with the mother liquor for a period of several days. Slowly, colorless, blue-emitting crystals were observed to be forming among the yellow, green-emitting crystals. These colorless crystals eventually grew to a size suitable for single-crystal X-ray diffraction. However, we noted that the transformation occurred at different rates depending on the anions present. For a 50/50 mixture of $(PF_6)^-$ and $(AsF_6)^-$, the transformation occurred in 1 or 2 days, whereas for a 50/50 mixture of $(PF_6)^-$ and $(SbF_6)^-$, the process took 1 month. For a 50/50 mixture of $(AsF_6)^-$ and $(SbF_6)^-$, it took 7 months for one colorless crystal to appear. Similarly, we noted that the colorless polymorph of $[(C_6H_{11}NC)_2Au](PF_6)$ could be formed by this process in 1 day, but it took 1 week to obtain the colorless polymorph of $[(C_6H_{11}NC)_2Au](AsF_6)$ in this fashion.

Structure and Properties of the Colorless, Blue-Emitting Crystals Obtained from a Mixture of Two Different Anions. Single-crystal X-ray diffraction data were obtained from nine different samples of various colorless crystals containing a mixture of two different anions, as set out in Table 2. As seen in Table 2, all of these crystals were isomorphous with one another and with the colorless polymorphs of $[(C_6H_{11}NC)_2Au](PF_6)$ and $[(C_6H_{11}NC)_2Au](AsF_6)$. On the crystallographic time scale, anions occupy common sites with fractional occupancy in the mixed-anion salts. The columnar structure of one salt, $[(C_6H_{11}NC)_2Au]$-

https://dx.doi.org/10.1021/jacs.9b13168
J. Am. Chem. Soc. 2020, 142, 5689−5701

Table 1. Crystallographic Data for Salts of $[(C_6H_{11}NC)_2Au]^+$

	$[(C_6H_{11}NC)_2Au](SbF_6)$	$[(C_6H_{11}NC)_2Au](PF_6)$[30]	$[(C_6H_{11}NC)_2Au](AsF_6)$[30]
color/habit	pale-yellow needle	colorless needle	colorless block
chemical formula	$C_{14}H_{22}AuF_6N_2Sb$	$C_{14}H_{22}AuF_6N_2P$	$C_{14}H_{22}AsAuF_6N_2$
formula weight	651.05	560.27	604.22
crystal system	monoclinic	monoclinic	monoclinic
space group	$P2_1/c$	$P2_1/c$	$P2_1/c$
a (Å)	24.761(3)	6.3644(5)	6.3965(15)
b (Å)	25.651(3)	16.9806(15)	17.194(4)
c (Å)	12.0706(14)	16.7224(13)	16.729(4)
α (deg)	90	90	90
β (deg)	97.011(2)	92.693(3)	92.658(8)
γ (deg)	90	90	90
V (Å^3)	7609.2(16)	1805.2(3)	1837.9(7)
Z	16	4	4
T (K)	100(2)	91(2)	90(2)
λ (Å)	0.71073	0.71073	0.71073
ρ (g/cm^3)	2.273	2.061	2.148
μ (mm^{-1})	9.177	8.264	9.847
R_1 (obsd data)[a]	0.0572	0.019	0.020
wR_2 (all data, F^2 refinement)[b]	0.1444	0.053	0.050

	$[(C_6H_{11}NC)_2Au]$-$(PF_6)_{0.25}(AsF_6)_{0.75}$	$[(C_6H_{11}NC)_2Au]$-$(PF_6)_{0.50}(AsF_6)_{0.50}$	$[(C_6H_{11}NC)_2Au]$-$(PF_6)_{0.75}(AsF_6)_{0.25}$
color/habit	colorless block	colorless block	colorless block
chemical formula	$C_{14}H_{22}As_{0.74}AuF_6N_2P_{0.26}$	$C_{14}H_{22}As_{0.50}AuF_6N_2P_{0.50}$	$C_{14}H_{22}As_{0.24}AuF_6N_2P_{0.76}$
formula weight	592.79	582.25	570.38
crystal system	monoclinic	monoclinic	monoclinic
space group	$P2_1/c$	$P2_1/c$	$P2_1/c$
a (Å)	6.3980(6)	6.3850(4)	6.3789(7)
b (Å)	17.152(2)	17.0891(12)	17.039(2)
c (Å)	16.741(2)	16.7204(11)	16.730(2)
α (deg)	90	90	90
β (deg)	92.747(4)	92.6860(10)	92.689(4)
γ (deg)	90	90	90
V (Å^3)	1835.0(4)	1822.4(2)	1816.4(4)
Z	4	4	4
T (K)	100(2)	100(2)	100(2)
λ (Å)	0.71073	0.71073	0.71073
ρ (g/cm^3)	2.146	2.122	2.089
μ (mm^{-1})	9.419	9.073	8.673
R_1 (obsd data)[a]	0.0222	0.0274	0.0241
wR_2 (all data, F^2 refinement)[b]	0.0595	0.0842	0.0648

	$[(C_6H_{11}NC)_2Au](PF_6)_{0.50}(SbF_6)_{0.50}$	$[(C_6H_{11}NC)_2Au](AsF_6)_{0.50}(SbF_6)_{0.50}$
color/habit	colorless block	colorless block
chemical formula	$C_{14}H_{22}AuF_6N_2P_{0.50}Sb_{0.50}$	$C_{14}H_{22}As_{0.50}AuF_6N_2Sb_{0.50}$
formula weight	605.66	627.64
crystal system	monoclinic	monoclinic
space group	$P2_1/c$	$P2_1/c$
a (Å)	6.4150(7)	6.4403(7)
b (Å)	17.2744(19)	17.4163(19)
c (Å)	16.7207(18)	16.7694(18)
α (deg)	90	90
β (deg)	92.713(2)	92.6590(15)
γ (deg)	90	90
V (Å^3)	1850.8(3)	1878.9(4)
Z	4	4
T (K)	100(2)	90(2)
λ (Å)	0.71073	0.71073
ρ (g/cm^3)	2.174	2.219
μ (mm^{-1})	8.761	9.461
R_1 (obsd data)[a]	0.0229	0.0185
wR_2 (all data, F^2 refinement)[b]	0.0768	0.0416

[a] $R_1 = (\sum||F_o| - |F_c||)/\sum|F_o|$. [b] $wR_2 = ((\sum[w(F_o^2 - F_c^2)^2])/\sum[w(F_o^2)^2])^{1/2}$.

https://dx.doi.org/10.1021/jacs.9b13168
J. Am. Chem. Soc. 2020, 142, 5689−5701

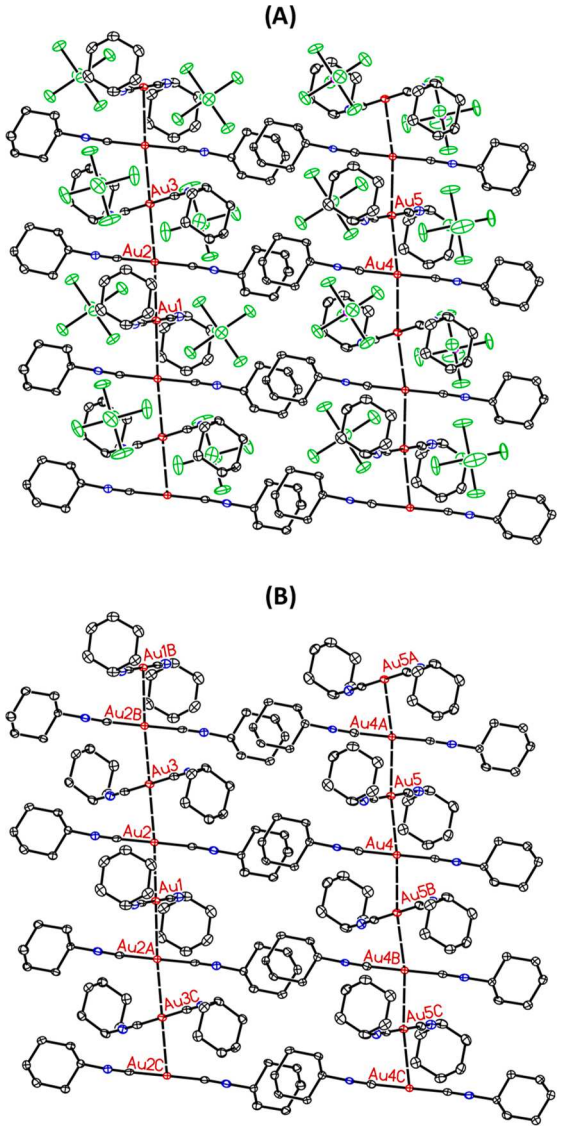

Figure 3. Drawings of the columnar structures within crystalline $[(C_6H_{11}NC)_2Au](SbF_6)$: (A) anions included and (B) anions removed. For clarity, hydrogen atoms are not shown. Aurophillic interactions are shown as dashed lines.

$(PF_6)_{0.50}(AsF_6)_{0.50}$, is shown in Figure 5. The gold ions reside on centers of symmetry. As seen in this figure, the cyclohexyl rings occupy alternating axial and equatorial positions along the chain of cations. Similar alternation of the axial and equatorial positioning of the cyclohexyl rings occurs in the structure of the yellow polymorphs of $[(C_6H_{11}NC)_2Au](PF_6)$ and $[(C_6H_{11}NC)_2Au](AsF_6)$.[30,31] The closest Au to F distance is 3.057 Å. Au1 has two such contacts, whereas Au2 has none. Not surprisingly, there are a number close C−H···F−P contacts, with the shortest being 2.341 Å.

The As:P ratios in these crystals were determined crystallographically with the occupancy of As and P allowed to refine freely. As the data in Table 2 show, the As:P ratio in the crystals reflects the As:P ratio in the solution used for crystal growth. Although previous studies of such mixed crystals have also shown that the compositions of the crystals and solutions from which they were grown were similar,[38] there are cases known where supramolecular selection occurs and the

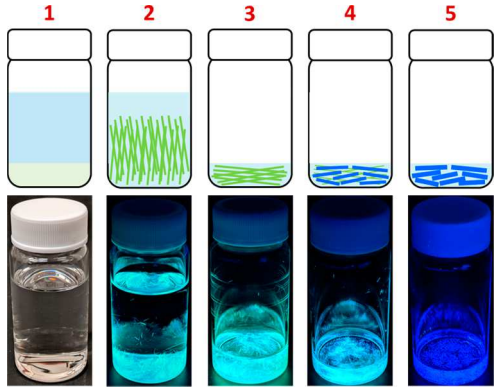

Figure 4. Formation of colorless, blue-emitting crystals of $[(C_6H_{11}NC)_2Au](PF_6)_{0.50}(AsF_6)_{0.50}$. In **1**, diethyl ether is carefully layered over a dichloromethane solution containing equimolar amounts of $[(C_6H_{11}NC)_2Au](PF_6)$ and $[(C_6H_{11}NC)_2Au](AsF_6)$. As the solutions diffuse together, yellow, greenish-emitting crystals form, as seen in **2** and **3**. For the ease of crystal removal, some of the mother liquor was removed to produce the sample in **3**. On standing, colorless, blue-emitting crystals begin to form, as seen in **4**. Eventually, the sample is dominated by the blue-emitting crystals shown in **5**. The photographs in **2**−**5** were taken under UV irradiation.

compositions of the crystals and the growth solutions differ.[39,40]

In general, the Au···Au distances for the salts of the type $[(C_6H_{11}NC)_2Au](PF_6)_n(AsF_6)_{1-n}$ fall between the Au···Au distances in $[(C_6H_{11}NC)_2Au](PF_6)$ (3.1822(3) Å) and $[(C_6H_{11}NC)_2Au](AsF_6)$ (3.1983(8) Å), with the Au···Au distances increasing as the As content of the crystals increases. Notice that the Au···Au distances in the antimony-containing crystals are even longer: 3.2075(4) Å for $[(C_6H_{11}NC)_2Au](PF_6)_{0.50}(SbF_6)_{0.50}$ and 3.2201(4) Å for $[(C_6H_{11}NC)_2Au](AsF_6)_{0.50}(SbF_6)_{0.50}$. Thus the presence of larger anions produces longer Au···Au distances in these crystals. However, the Au···Au distances in all of these colorless, blue-emitting salts are longer than the corresponding distances in $[(C_6H_{11}NC)_2Au](SbF_6)$ and in the yellow polymorphs of $[(C_6H_{11}NC)_2Au](PF_6)$ and $[(C_6H_{11}NC)_2Au](AsF_6)$.

The presence of two different anions in these crystals has been confirmed by infrared spectroscopy. Figure 6 compares the infrared spectrum of the colorless mixed-anion salt $[(C_6H_{11}NC)_2Au](PF_6)_{0.50}(AsF_6)_{0.50}$ with those of colorless polymorphs of $[(C_6H_{11}NC)_2Au](PF_6)$ and $[(C_6H_{11}NC)_2Au](AsF_6)$. The infrared spectrum of a single crystal of $[(C_6H_{11}NC)_2Au](PF_6)_{0.50}(AsF_6)_{0.50}$ shows both P−F vibrations at 828 and 556 cm^{-1} and As−F vibrations at 687 and 392 cm^{-1}. Similar infrared spectra have been obtained for the other salts shown in Table 2.

Figure 7 shows the emission and excitation spectra of a colorless, blue-emitting polycrystalline sample of $[(C_6H_{11}NC)_2Au](PF_6)_{0.50}(SbF_6)_{0.50}$.

Properties of the Yellow, Green-Emitting Crystals Obtained from a Mixture of Two Different Anions. Unfortunately, all of the yellow crystals with green emission that formed from a mixture of two anions were too small for single-crystal X-ray diffraction. However, powder X-ray diffraction data have been obtained for these yellow crystals derived from a mixture of two different anions. For simplicity, we will refer to the yellow crystals grown from a solution of equimolar amounts of $[(C_6H_{11}NC)_2Au](PF_6)$ and $[(C_6H_{11}NC)_2Au](AsF_6)$ as yellow $[(C_6H_{11}NC)_2Au]$-

https://dx.doi.org/10.1021/jacs.9b13168
J. Am. Chem. Soc. 2020, 142, 5689−5701

Table 2. Comparison of Properties of Mixed-Anion Salts of $[(C_6H_{11}NC)_2Au]^+$ from X-ray Crystallography

		R_1 (%)	Au1···Au2 distance (Å)
As:P ratio in solution	As:P ratio from SC-XRD		
ll85 0.75:0.25	0.735(2):0.265(2)	2.22	3.1990(3)
ll92 0.75:0.25	0.729(2):0.281(2)	2.41	3.1965(3)
ll58 0.50:0.50	0.485(2):0.515(2)	2.78	3.1933(4)
ll94 0.50:0.50	0.474(2):0.526(2)	2.74	3.1925(2)
ll86 0.25:0.75	0.243(2):0.757(2)	2.41	3.1895(4)
ll90 0.25:0.75	0.243(2):0.757(2)	2.50	3.1887(3)
ll89 0.25:0.75	0.235(3):0.765(3)	3.13	3.1864(5)
Sb:As ratio in solution	Sb:As ratio from SC-XRD		
0.50:0.50	0.466(3):0.534(3)	2.45	3.2201(4)
Sb:P ratio in solution	Sb:P ratio from SC-XRD		
0.50:0.50	0.492(1):0.508(1)	2.29	3.2075(4)
$[(C_6H_{11}NC)_2Au](PF_6)$	see ref 30		3.1822(3)
$[(C_6H_{11}NC)_2Au](AsF_6)$	see ref 31		3.1983(8)

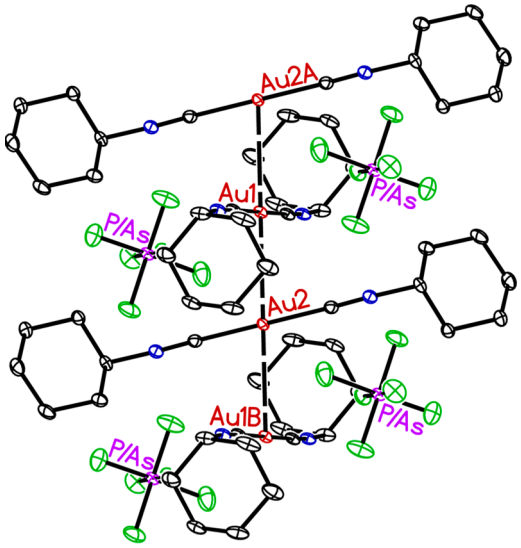

Figure 5. Columnar structure within colorless, crystalline $[(C_6H_{11}NC)_2Au](PF_6)_{0.50}(AsF_6)_{0.50}$. For clarity, hydrogen atoms are not shown. Aurophillic interactions are shown as dashed lines.

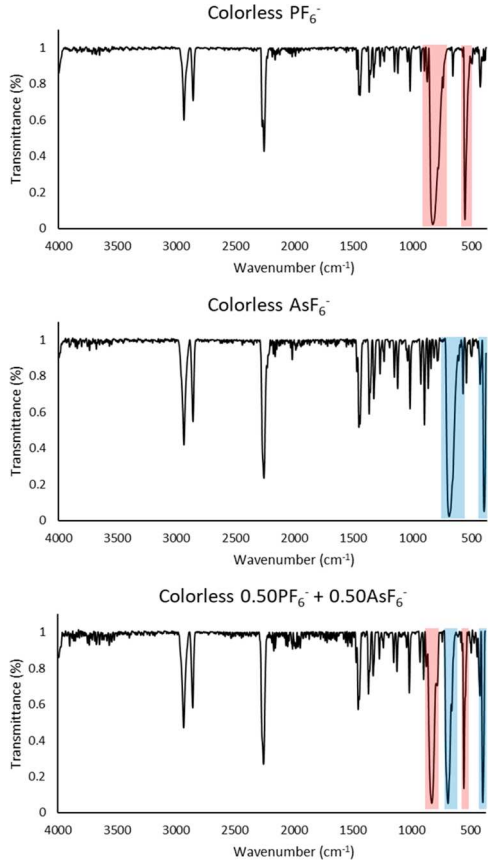

Figure 6. Infrared spectra of crystals of $[(C_6H_{11}NC)_2Au](PF_6)$ and $[(C_6H_{11}NC)_2Au](AsF_6)$ and a single crystal of $[(C_6H_{11}NC)_2Au](PF_6)_{0.5}(AsF_6)_{0.5}$. The P−F vibrations at 828 and 556 cm^{-1} are highlighted in pink, and the As−F vibrations at 687 and 392 cm^{-1} are highlighted in blue.

$(PF_6)_{0.50}(AsF_6)_{0.50}$ and will use similar nomenclature for other yellow mixed-anion crystals. We realize that this nomenclature makes the assumption that the composition of crystals reflects the composition of the solution from which they are grown, an assumption that can have exceptions.[34−36]

Figure 8 compares the X-ray powder diffraction from yellow $[(C_6H_{11}NC)_2Au](PF_6)_{0.50}(AsF_6)_{0.50}$ with those of yellow $[(C_6H_{11}NC)_2Au](PF_6)$ and yellow $[(C_6H_{11}NC)_2Au](AsF_6)$. The data suggest that there is no evidence of the presence of $[(C_6H_{11}NC)_2Au](AsF_6)$ in the mixed-anion sample. However, the powder pattern of the mixed-anion sample is similar to that of yellow $[(C_6H_{11}NC)_2Au](PF_6)$. The powder pattern for $[(C_6H_{11}NC)_2Au](PF_6)_{0.50}(AsF_6)_{0.50}$ contains almost each peak seen in the powder pattern for $[(C_6H_{11}NC)_2Au](PF_6)$, with some changes in relative intensity. The yield of the process that gives the mixed-anion sample is 97%, which indicates that the sample cannot be exclusively yellow $[(C_6H_{11}NC)_2Au](PF_6)$. Rather, we suggest that the mixed-anion sample is isomorphic with yellow $[(C_6H_{11}NC)_2Au](PF_6)$ but with the replacement of half of the $(PF_6)^-$ ions with $(AsF_6)^-$ and some adjustments in the separations between cations. Additionally, the infrared spectrum taken from one crystal of yellow $[(C_6H_{11}NC)_2Au](PF_6)_{0.50}(AsF_6)_{0.50}$ revealed the presence of P−F vibrations at 838 and 558 cm^{-1} and As−F vibrations at 699 and 393 cm^{-1}.

To further identify the composition of the mixed crystals, mass spectroscopic studies were performed. One crystal of yellow $[(C_6H_{11}NC)_2Au](PF_6)_{0.50}(AsF_6)_{0.50}$ was transferred to a vial and dissolved in 0.5 mL of acetonitrile. A 5 μL aliquot of the solution was examined by negative-mode electrospray ionization mass spectrometry (ESI-MS) after an initial 5 μL of acetonitrile control run. A peak at m/z of 145.0 corresponds to the $(PF_6)^-$ anion, whereas the second peak at m/z of 188.8

https://dx.doi.org/10.1021/jacs.9b13168
J. Am. Chem. Soc. 2020, 142, 5689−5701

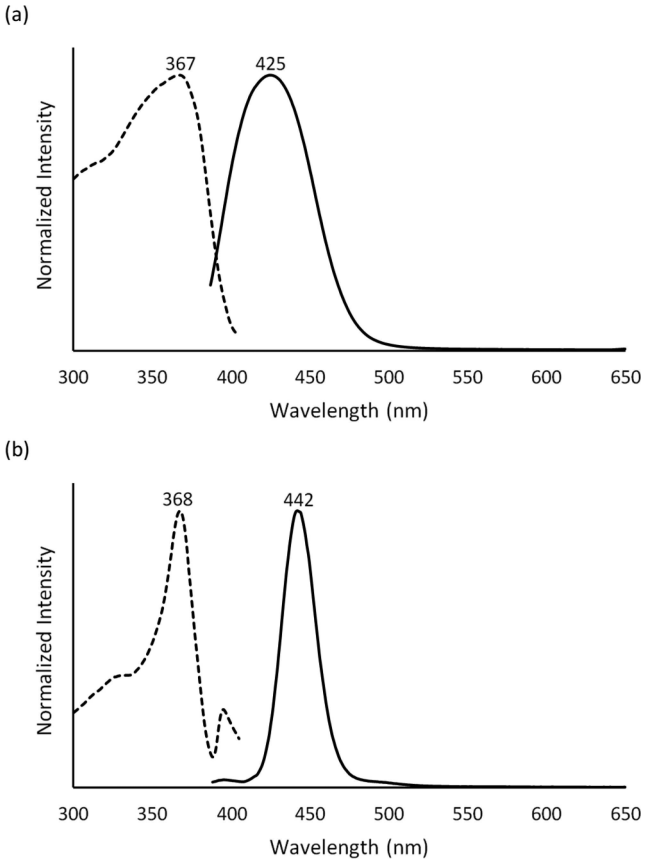

Figure 7. Emission and excitation spectra of a colorless, blue-emitting polycrystalline sample of $[(C_6H_{11}NC)_2Au](PF_6)_{0.50}(SbF_6)_{0.50}$ at (a) 298 and (b) 77 K.

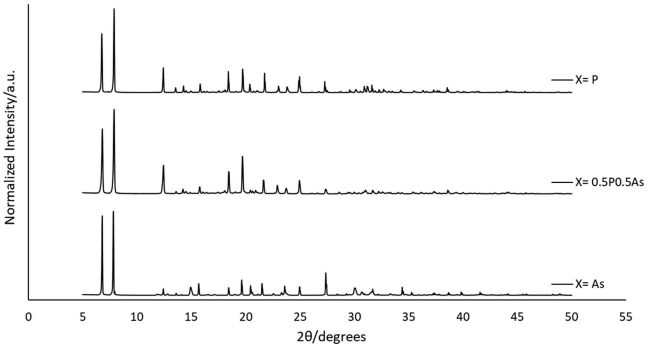

Figure 8. Comparison of X-ray powder diffraction data for: (top) yellow $[(C_6H_{11}NC)_2Au](PF_6)$, (middle) yellow $[(C_6H_{11}NC)_2Au](PF_6)_{0.50}(AsF_6)_{0.50}$, and (bottom) yellow $[(C_6H_{11}NC)_2Au](AsF_6)$ at 298 K.

corresponds to the $(AsF_6)^-$ anion. Thus both anions are present in the yellow mixed-anion crystal. The normalized relative intensity does not necessarily relate to the ratio of anions in the complex because the ionization efficiency of each anion may differ. A control acetonitrile solution of equal molar ratios of $(NH_4)(PF_6)$ and $Na(AsF_6)$ showed the same relative intensities (1:1.59) for the 145.0 and 188.8 peaks as seen for the yellow crystal.

The X-ray powder diffraction data for yellow crystals obtained from a mixture of $[(C_6H_{11}NC)_2Au](PF_6)$ and $[(C_6H_{11}NC)_2Au](SbF_6)$ are similar, as seen in the Supporting Information. The powder pattern for the $[(C_6H_{11}NC)_2Au](PF_6)_{0.50}(SbF_6)_{0.50}$ crystals also resembles that of yellow $[(C_6H_{11}NC)_2Au](PF_6)$. The presence of both $(PF_6)^-$ and $(SbF_6)^-$ in a single crystal of $[(C_6H_{11}NC)_2Au](PF_6)_{0.50}(SbF_6)_{0.50}$ was established by mass spectroscopic studies. A single crystal of yellow $[(C_6H_{11}NC)_2Au](PF_6)_{0.50}(SbF_6)_{0.50}$ produced negative-mode ESI-MS peaks at m/z 145.0 for the $(PF_6)^-$ anion and two peaks at m/z 234.8 and 236.8 for the $(SbF_6)^-$ anion.

The X-ray powder diffraction from yellow $[(C_6H_{11}NC)_2Au](AsF_6)_{0.50}(SbF_6)_{0.50}$ is compared with those of yellow $[(C_6H_{11}NC)_2Au](AsF_6)$ and yellow $[(C_6H_{11}NC)_2Au](SbF_6)$ in Figure 9. In this case, the powder

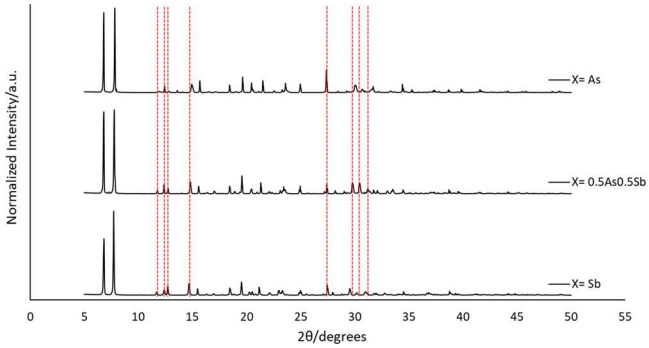

Figure 9. Comparison of X-ray powder diffraction data for: top, yellow $[(C_6H_{11}NC)_2Au](AsF_6)$; middle, yellow $[(C_6H_{11}NC)_2Au](AsF_6)_{0.50}(SbF_6)_{0.50}$; and bottom, yellow $[(C_6H_{11}NC)_2Au](SbF_6)$.

pattern from yellow $[(C_6H_{11}NC)_2Au](AsF_6)_{0.50}(SbF_6)_{0.50}$ is different from those of pure yellow $[(C_6H_{11}NC)_2Au](AsF_6)$ or yellow $[(C_6H_{11}NC)_2Au](SbF_6)$. The vertical red lines draw attention to places where the two powder patterns differ. It appears that a new phase (or phases) is present in yellow $[(C_6H_{11}NC)_2Au](AsF_6)_{0.50}(SbF_6)_{0.50}$. A single crystal of yellow $[(C_6H_{11}NC)_2Au](AsF_6)_{0.50}(SbF_6)_{0.50}$ produced negative-mode ESI-MS peaks at m/z 188.8 for the $(AsF_6)^-$ anion and two peaks at m/z 234.8 and 236.8 for the $(SbF_6)^-$ anion.

The emission and excitation λ_{max} values from the spectra for the colorless and yellow crystals are given in Table 3. These yellow crystals exhibit an emission maximum in the 480−490 nm region at 298 K. On cooling, the emission spectrum of each yellow form shows two distinct maxima. Figure 10 compares the emission and excitation spectra taken at 77 K for the yellow, green-emitting crystals of $[(C_6H_{11}NC)_2Au](PF_6)_{0.50}(AsF_6)_{0.50}$ and $[(C_6H_{11}NC)_2Au](PF_6)_{0.50}(SbF_6)_{0.50}$, with similar spectra for the pure phase, $[(C_6H_{11}NC)_2Au](PF_6)$. The emission spectra of $[(C_6H_{11}NC)_2Au](PF_6)_{0.50}(AsF_6)_{0.50}$ and $[(C_6H_{11}NC)_2Au](PF_6)_{0.50}(SbF_6)_{0.50}$ do not show features at 509 and 554 nm that should be present if a significant amount of pure $[(C_6H_{11}NC)_2Au](PF_6)$ was present. Thus we suggest that new phases are present in the samples with mixed anions. This conclusion is consistent with the X-ray powder data, which suggested that the yellow crystals of $[(C_6H_{11}NC)_2Au](PF_6)_{0.50}(AsF_6)_{0.50}$ and $[(C_6H_{11}NC)_2Au](PF_6)_{0.50}(SbF_6)_{0.50}$ produced distinct diffraction data that suggested that their structures were similar to that of the yellow polymorph of $[(C_6H_{11}NC)_2Au](PF_6)$.

Exposure of samples of the yellow forms of $[(C_6H_{11}NC)_2Au](PF_6)_{0.75}(AsF_6)_{0.25}$, $[(C_6H_{11}NC)_2Au](PF_6)_{0.50}(AsF_6)_{0.50}$, and $[(C_6H_{11}NC)_2Au](PF_6)_{0.25}(AsF_6)_{0.75}$ to vapors of methanol or dichloromethane results in a change in color to colorless and a change in emission from blue to

https://dx.doi.org/10.1021/jacs.9b13168
J. Am. Chem. Soc. 2020, 142, 5689−5701

Table 3. Emission and Excitation Maxima for Salts of $[(C_6H_{11}NC)_2Au]^+$

anion composition	emission λ_{max} (nm), 298 K	lifetime (μs), 298 K	excitation λ_{max} (nm), 298 K	emission λ_{max} (nm), 77 K	excitation λ_{max} (nm), 77 K	lifetime (μs), 77 K
Colorless						
(PF_6)	425	8.1	357	442	378	11.5
$(PF_6)_{0.75}(AsF_6)_{0.25}$	427	8.7	354	441	372	9.2
$(PF_6)_{0.50}(AsF_6)_{0.50}$	426	8.9	355	443	374	10.4
$(PF_6)_{0.25}(AsF_6)_{0.75}$	429	8.7	368	436	369	9.6
(AsF_6)	422	8.1	358	438	370	11.5
$(PF_6)_{0.50}(SbF_6)_{0.50}$	425	8.3	367	442	368	8.8
$(AsF_6)_{0.50}(SbF_6)_{0.50}$	424	8.9	352	439	373	9.1
Yellow						
(PF_6)	481	6.3	397	509, 554	450	8.3, 8.2
$(PF_6)_{0.75}(AsF_6)_{0.25}$	482	6.6	419	507, 554	461, 449	9.0, 8.8
$(PF_6)_{0.50}(AsF_6)_{0.50}$	482	6.7	419	502, 549	449, 457	9.7, 9.8
$(PF_6)_{0.25}(AsF_6)_{0.75}$	482	6.8	419	492, 538	436, 419	8.4, 8.2
(AsF_6)	485	7.4	419	486, 531	438	8.3, 8.0
$(PF_6)_{0.50}(SbF_6)_{0.50}$	490	7.5	419	489, 536	443, 430	9.6, 9.5
$(AsF_6)_{0.50}(SbF_6)_{0.50}$	484	7.4	419	479, 522	439, 372	8.1, 8.6
(SbF_6)	476	6.8	398	452, 495	421, 368	8.4, 8.6

green. These changes are analogous to the effects of vapor on crystals of the yellow polymorphs of $[(C_6H_{11}NC)_2Au](PF_6)$ and $[(C_6H_{11}NC)_2Au](AsF_6)$, as previously reported.[30,31] However, the yellow crystals of $[(C_6H_{11}NC)_2Au](PF_6)_{0.50}(SbF_6)_{0.50}$ and $[(C_6H_{11}NC)_2Au](AsF_6)_{0.50}(SbF_6)_{0.50}$ do not undergo any change in color or emission when exposed to vapors of methanol or dichloromethane.

Trace A of Figure 11 shows the X-ray powder diffraction data for a yellow sample of $[(C_6H_{11}NC)_2Au](PF_6)_{0.50}(AsF_6)_{0.50}$, as grown from solution. Trace B shows the diffraction data for a yellow sample of $[(C_6H_{11}NC)_2Au](PF_6)_{0.50}(AsF_6)_{0.50}$ after exposure to dichloromethane vapor, which has converted the sample into a colorless, blue-emitting solid. Trace C shows the X-ray powder diffraction data for crystals of colorless $[(C_6H_{11}NC)_2Au](PF_6)_{0.50}(AsF_6)_{0.50}$ that were grown from solution. Notice that the powder patterns seen in Traces B and C are virtually identical, which shows that vapor transformed the yellow sample of $[(C_6H_{11}NC)_2Au](PF_6)_{0.50}(AsF_6)_{0.50}$ into the colorless form.

Thermochromic Behavior of Colorless, Blue-Emitting Crystals of Mixed-Anion Salts. Of all five different forms of the single-anion crystals, colorless and yellow $[(C_6H_{11}NC)_2Au](PF_6)$, colorless and yellow $[(C_6H_{11}NC)_2Au](AsF_6)$, and pale-yellow $[(C_6H_{11}NC)_2Au](SbF_6)$, only the colorless form of $[(C_6H_{11}NC)_2Au](AsF_6)$ is thermochromic. Remarkably, all of the colorless crystals formed from a mixture of two anions show luminescence thermochromism. Upon heating to a temperature below their melting points, each type of crystal shows a change in luminescence from the blue of the colorless crystals to green. The process is irreversible. Upon cooling, the green persists. Moreover, the cooled samples retain their green luminescence when stored for periods as long as 1 year.

Figure 12 shows a photograph taken under UV irradiation of a single crystal of colorless, blue-emitting $[(C_6H_{11}NC)_2Au](PF_6)_{0.50}(AsF_6)_{0.50}$ before and after heating to 104−108 °C. A video of the process is shown in the Supporting Information. The sample does not melt at this temperature, and it retains its external morphology. Whereas the initial sample was a single crystal, the yellow, green-emitting solid that is produced upon warming no longer shows X-ray diffraction, consistent with a single-crystal to single-crystal transformation. However, X-ray powder diffraction data show that the thermal transformation results in the formation of the yellow, green-emitting salt. Trace C of Figure 11 shows the powder pattern for the colorless crystals of $[(C_6H_{11}NC)_2Au](PF_6)_{0.50}(AsF_6)_{0.50}$, whereas Trace D shows the powder diffraction obtained from colorless crystals after heating to 108 °C. The data in Trace D are virtually identical to those of the yellow crystals of $[(C_6H_{11}NC)_2Au](PF_6)_{0.50}(AsF_6)_{0.50}$ that are obtained from solution, as seen in Trace A of Figure 11.

Table 4 presents the temperatures for the thermochromic process and the melting points for the crystals considered here. It is particularly interesting to note that the colorless form of $[(C_6H_{11}NC)_2Au](PF_6)_{0.50}(SbF_6)_{0.50}$ is thermochromic, whereas neither polymorph of $[(C_6H_{11}NC)_2Au](PF_6)$ nor $[(C_6H_{11}NC)_2Au](SbF_6)$ is thermochromic. Also, the temperatures at which the individual crystals undergo their change in emission vary as the anion compositions are altered. Notice that the temperature required to transform a crystal of the type $[(C_6H_{11}NC)_2Au](PF_6)_n(AsF_6)_{1-n}$ from colorless (blue-emitting) to yellow (green-emitting) decreases as the fraction of hexafluoroarsenate ion in the crystal increases, as shown in Figure 13. These thermochromic changes are all irreversible.

The thermochromic behavior of the various colorless crystals listed in Table 4 has been monitored by following the emission and excitation spectra of the salts. Figure 14 shows emission and excitation spectra from crystals of $[(C_6H_{11}NC)_2Au](PF_6)_{0.50}(SbF_6)_{0.50}$ at 77 K. Trace (a) shows the spectrum for the colorless crystals before heating. Trace (b) shows the spectrum obtained after the sample was warmed to 104−108 °C but not heated to the higher temperature where melting occurs. After heating, the sample was first allowed to cool to room temperature and subsequently cooled to 77 K for spectroscopic work. At this point, the sample was yellow under ambient light. Trace (c) shows data for a sample of the yellow $[(C_6H_{11}NC)_2Au](PF_6)_{0.50}(SbF_6)_{0.50}$ produced by crystallization from solution. Notice the similarity of the spectra in Traces (b) and (c). Figure 15 shows a similar set of data for crystals of $[(C_6H_{11}NC)_2Au](AsF_6)_{0.50}(SbF_6)_{0.50}$. Again, notice that the spectra of the colorless compound after heating correspond

https://dx.doi.org/10.1021/jacs.9b13168
J. Am. Chem. Soc. 2020, 142, 5689−5701

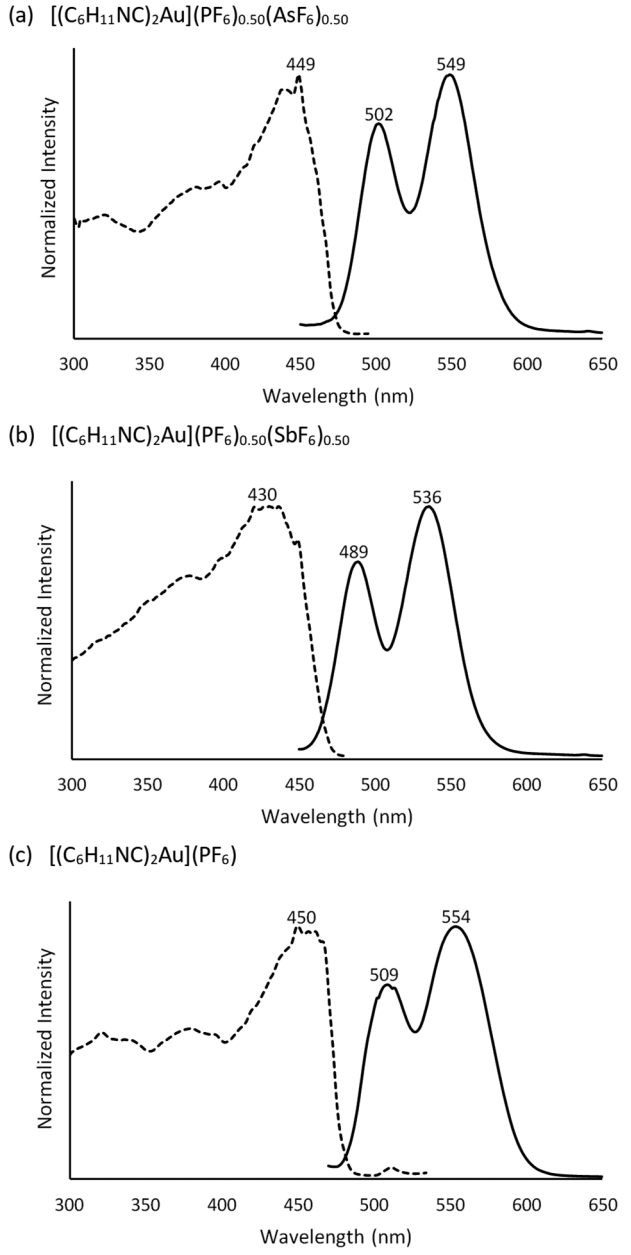

Figure 10. Emission and excitation spectra of yellow, green-emitting crystals of (a) $[(C_6H_{11}NC)_2Au](PF_6)_{0.50}(AsF_6)_{0.50}$, (b) $[(C_6H_{11}NC)_2Au](PF_6)_{0.50}(SbF_6)_{0.50}$, and (c) $[(C_6H_{11}NC)_2Au](PF_6)$ at 77 K.

rather well to the spectra of the yellow crystals obtained directly from solution.

Mechanochromic Behavior. None of the salts reported here showed any changes in color or luminescence when subjected to grinding.

DISCUSSION

A number of new crystalline forms of the two-coordinate cation, $[(C_6H_{11}NC)_2Au]^+$, have been prepared. All are intensely luminescent with emission that comes in various shades of blue or green and is readily detected by the human eye. The luminescence is associated with the formation of extended aurophilic interactions in the solid state. Within the chain, electronic excitation occurs to promote an electron from the filled d orbital band to the empty p orbital band, whereas

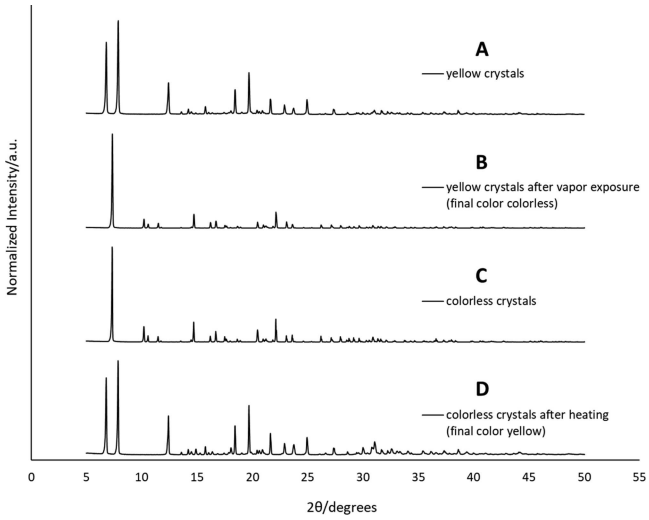

Figure 11. Comparison of X-ray powder diffraction data for: (A) yellow crystals of $[(C_6H_{11}NC)_2Au](PF_6)_{0.50}(AsF_6)_{0.50}$, (B) colorless crystals obtained by the exposure of yellow crystals of $[(C_6H_{11}NC)_2Au](PF_6)_{0.50}(AsF_6)_{0.50}$ to dichloromethane vapor, (C) colorless crystals of $[(C_6H_{11}NC)_2Au](PF_6)_{0.50}(AsF_6)_{0.50}$ obtained from solution, and (d) yellow crystals obtained after heating colorless crystals of $[(C_6H_{11}NC)_2Au](PF_6)_{0.50}(AsF_6)_{0.50}$ to 108 °C.

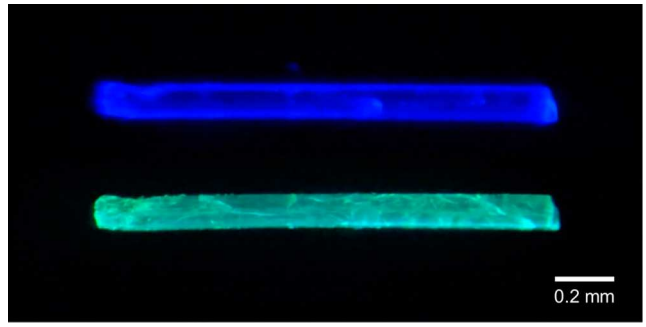

Figure 12. Photographs of the luminescence from a crystal of $[(C_6H_{11}NC)_2Au](PF_6)_{0.50}(AsF_6)_{0.50}$. Top: blue luminescence before heating to 104−108 °C. Bottom: green luminescence after heating.

Table 4. Thermochromic and Melting Point Ranges

compound	thermochromic range (°C)	melting point range (°C)
Colorless Form		
$[(C_6H_{11}NC)_2Au](PF_6)$	none	115−120
$[(C_6H_{11}NC)_2Au](AsF_6)$	98−102	123−125
$[(C_6H_{11}NC)_2Au](PF_6)_{0.50}(SbF_6)_{0.50}$	87−95	114−116
$[(C_6H_{11}NC)_2Au](AsF_6)_{0.50}(SbF_6)_{0.50}$	88−92	113−114
$[(C_6H_{11}NC)_2Au](PF_6)_{0.50}(AsF_6)_{0.50}$	104−108	118−119
$[(C_6H_{11}NC)_2Au](PF_6)_{0.75}AsF_6)_{0.25}$	105−111	118−121
$[(C_6H_{11}NC)_2Au](PF_6)_{0.25}(AsF_6)_{0.75}$	100−105	118−121
Yellow Form		
$[(C_6H_{11}NC)_2Au](PF_6)$	none	110−115
$[(C_6H_{11}NC)_2Au](AsF_6)$	none	123−126
$[(C_6H_{11}NC)_2Au](SbF_6)$	none	113−115

the emission occurs via the reverse process.[21] In solution, where these chains dissociate to form monomers, there is no emission. Note that the related salt, $[(CH_3NC)_2Au](PF_6)$, which has anions immediately surrounding the isolated cation, is colorless and nonemissive.[30]

https://dx.doi.org/10.1021/jacs.9b13168
J. Am. Chem. Soc. 2020, 142, 5689−5701

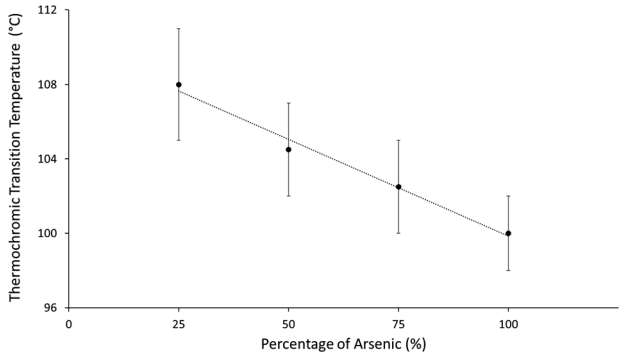

Figure 13. Thermochromic transition temperature range as a function of the percentage of $(AsF_6)^-$ present in the mixed crystals of $[(C_6H_{11}NC)_2Au](PF_6)_n(AsF_6)_{1-n}$.

Our results show that the properties and structures of salts of the two-coordinate cation, $[(C_6H_{11}NC)_2Au]^+$, vary significantly based on the identity of the anion present, even though the anion is noncoordinating and geometrically well away from the chains of gold(I) ions that run through the crystals. Moreover, crystals containing two different anions can have properties that are lacking in the two counterpart salts that involve only a single anion. For example, the colorless form of $[(C_6H_{11}NC)_2Au](PF_6)_{0.50}(SbF_6)_{0.50}$ is thermochromic, whereas neither polymorph of $[(C_6H_{11}NC)_2Au](PF_6)$ nor $[(C_6H_{11}NC)_2Au](SbF_6)$ is thermochromic. Additionally, the colorless forms of $[(C_6H_{11}NC)_2Au](PF_6)_{0.50}(SbF_6)_{0.50}$ and $[(C_6H_{11}NC)_2Au](AsF_6)_{0.50}(SbF_6)_{0.50}$ contain linear chains of gold(I) ions, whereas $[(C_6H_{11}NC)_2Au](SbF_6)$ is pale-yellow and contains somewhat kinked chains of gold(I) ions. Finally, all of the mixed-anion salts reported here including those containing $(SbF_6)^-$ form both colorless and yellow crystals, whereas $[(C_6H_{11}NC)_2Au](SbF_6)$ forms only pale-yellow crystals.

Through the formation of mixed-anion containing crystals, we have been able to expand the number of luminescent thermochromic crystals to include the five new compounds reported in Table 4. In these crystals, the luminescent thermochromic transition occurs at distinct temperature ranges that vary from 87−95 to 105−111 °C. The temperature required to transform a crystal of the type $[(C_6H_{11}NC)_2Au](PF_6)_n(AsF_6)_{1-n}$ from colorless (blue-emitting) to yellow (green-emitting) decreases as the fraction of hexafluoroarsenate ion in the crystal increases. In each case, the colorless, blue-emitting crystals are converted into a yellow, green-emitting solid in an irreversible process.

The anions appear to influence the structure of these salts because of the differences in their volumes, which increase as the size of the central atom increases in order: $(PF_6)^-$ < $(AsF_6)^-$ < $(SbF_6)^-$. Using our experimental P−F distances and the van der Waals radius of fluorine with a simple octahedral model, the volume of $(PF_6)^-$ is 38 Å^3. Similarly, the volumes of $(AsF_6)^-$ and $(SbF_6)^-$ are 43 and 49 Å^3. As an example of this effect, notice that the Au···Au separation along a chain of cations in the colorless polymorphs increases as the sizes of the anions increase, as seen in Table 2. Similarly, the Au···Au separations in the yellow crystals also increase as the sizes of the anions increase. Differences in the volumes of the anions are also likely to be responsible for the variation in the thermochromic and vapochromic responses of the various crystals reported here. Ultimately, the anions influence the aurophilic interactions within each salt. Those aurophilic interactions alone provide the chromophores that are responsible of the optical properties of these crystals.

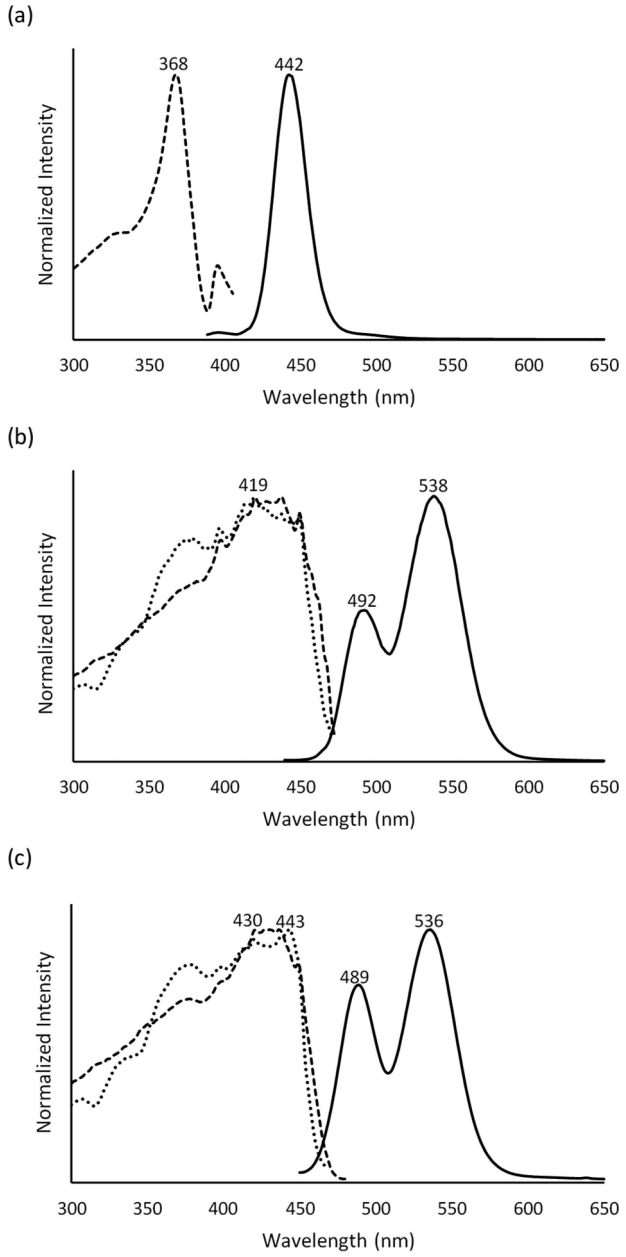

Figure 14. Emission and excitation spectra of crystals of $[(C_6H_{11}NC)_2Au](PF_6)_{0.50}(SbF_6)_{0.50}$ at 77 K. (a) Excitation (dashed) at 442 nm and emission (solid) at 368 nm of colorless $[(C_6H_{11}NC)_2Au](PF_6)_{0.50}(SbF_6)_{0.50}$. (b) Excitation (dashed) at 538 nm, excitation (dotted) at 492 nm, and emission (solid) at 419 nm of the yellow solid obtained by heating colorless $[(C_6H_{11}NC)_2Au](PF_6)_{0.50}(SbF_6)_{0.50}$ to 87−95 °C and then cooling. (c) Excitation (dashed) at 537 nm, excitation (dotted) at 490 nm, and emission (solid) at 419 nm of yellow crystals of $[(C_6H_{11}NC)_2Au](PF_6)_{0.50}(SbF_6)_{0.50}$ obtained from solution at 77 K.

EXPERIMENTAL SECTION

Materials. Foul smelling cyclohexyl isocyanide is toxic and must be handled in a well-ventilated fume hood. Samples of cyclohexyl isocyanide were purchased from Acros Organics and used as received. Chloro(tetrahydrothiophene)gold(I) was prepared by an established

https://dx.doi.org/10.1021/jacs.9b13168
J. Am. Chem. Soc. 2020, 142, 5689−5701

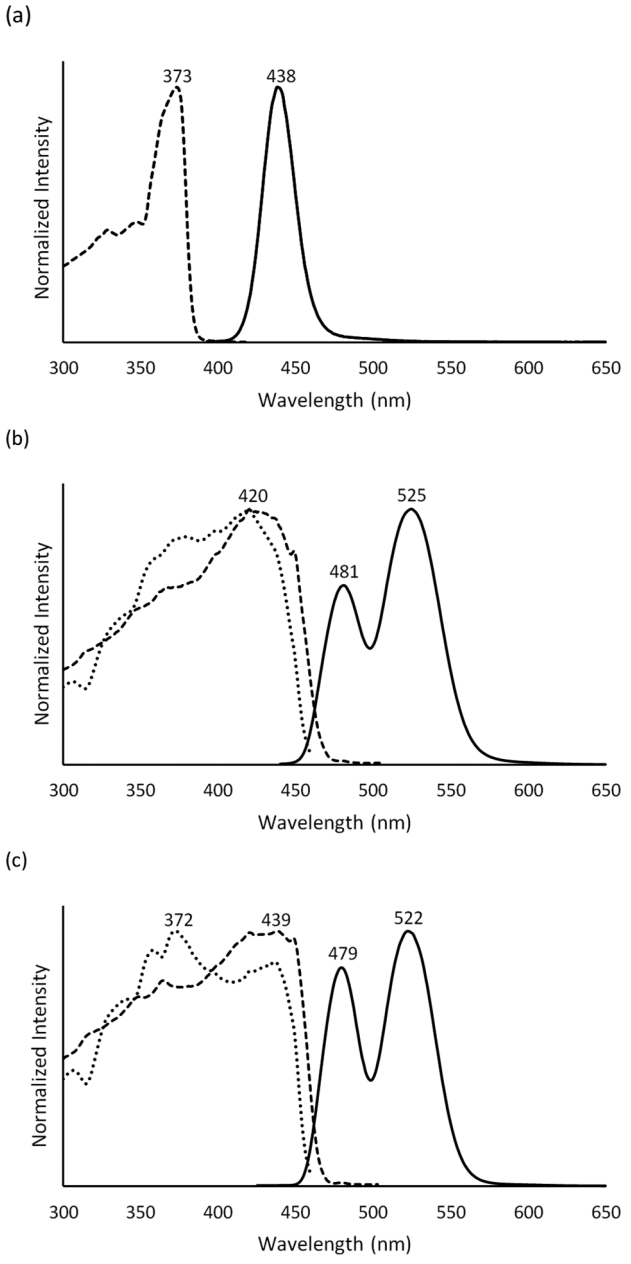

Figure 15. Emission and excitation spectra of crystals of $[(C_6H_{11}NC)_2Au](AsF_6)_{0.50}(SbF_6)_{0.50}$ at 77 K. (a) Colorless crystals obtained from solution: excitation (dashed) for emission at 440 nm and emission (solid) with excitation at 373 nm. (b) Yellow crystals obtained by heating the colorless crystals to 88−92 °C without melting: excitation (dashed) for emission at 480 nm, excitation (dotted) for emission at 525 and emission (solid) at with excitation at 420 nm. (c) Yellow crystals of $[(C_6H_{11}NC)_2Au](AsF_6)_{0.50}(SbF_6)_{0.50}$ obtained by growth from solution: excitation (dashed) for emission at 480 nm, excitation (dotted) for emission at 522 and emission (solid) with excitation at 372 nm.

method.[41] Samples of $[(C_6H_{11}NC)_2Au](PF_6)$[30] and of $[(C_6H_{11}NC)_2Au](AsF_6)$[31] were prepared as previously described.

Preparation of $[(C_6H_{11}NC)_2Au](SbF_6)$. A 20 mL vial was charged with 0.1514 g (0.472 mmol) of chloro(tetrahydrothiophene)gold(I), 0.1063 g (0.974 mmol) of $C_6H_{11}NC$ (cyclohexyl isocyanide), and 8 mL of acetonitrile while stirring. Once homogeneous (~10 min), 0.1342 g (0.519 mmol) of $Na(SbF_6)$ in 10 mL of acetonitrile was added. The combined mixture was stirred for 30 s and filtered, and the volatiles were removed by rotary evaporation. The resulting yellow oil was dissolved in 5 mL of dichloromethane and filtered through a short pad of celite. Diethyl ether was then added to precipitate 0.2627 g (0.403 mmol) of $[(C_6H_{11}NC)_2Au](SbF_6)$ as a pale-yellow solid (85%). ^{1}H NMR (400 MHz, $CDCl_3$, 25 °C): δ 4.10 (m, 2H), 2.02 (m, 4H), 1.80 (m, 4H), 1.69 (m, 4H), 1.46 (m, 4H), 1.42 (m, 4H). $^{13}C\{^1H\}$ NMR (100 MHz, $CDCl_3$, 25 °C): δ 138.6, 56.0, 31.4, 24.5, 22.8. UV (CH_2Cl_2) λ_{max}, nm (ε): 216 (9351), 238 (3050), 244 (3367). IR: 2934, 2866, 2846, 2261, 1455 cm^{-1}.

Crystallization of $[(C_6H_{11}NC)_2Au](SbF_6)$. A 0.0100 g (0.0154 mmol) sample of $[(C_6H_{11}NC)_2Au](SbF_6)$ powder was dissolved in 0.5 mL of dichloromethane. The filtered solution was transferred to a vial. An addition of 1.5 mL of diethyl ether was mixed with the dichloromethane solution. A 6 mL portion of diethyl ether was then carefully layered over the dichloromethane/diethyl ether solution. The vial was capped for slow diffusion to occur. Crystallization of needles of the product occurred almost immediately. In solution the crystals appeared colorless, but once dry, the crystals were pale-yellow in color. Under a UV lamp, these crystals displayed a blue luminescence. The pale-yellow, blue-luminescent crystals melted from 113 to 115 °C. No color or luminescence changes occurred during heating. The melt appeared colorless and was still blue-luminescent. When solidified, the pale-yellow color returned, and the blue luminescence was still present.

Production of the Salts Incorporating Two Different Anions. The mixed-anion salts were prepared from a mixture of the two individual salts by using the method shown in Figure 4. The process started by layering 14 mL of diethyl ether over 1 mL of a 71.4 mM solution of the two salts.

X-ray Crystallography and Data Collection. All crystals were transferred with a small amount of mother liquor to a microscope slide and immediately coated with a hydrocarbon oil. A suitable crystal of each compound, except for $[(C_6H_{11}NC)_2Au](AsF_6)_{0.50}(SbF_6)_{0.50}$, was mounted in the 100 K nitrogen cold stream provided by an Oxford Cryostream low-temperature apparatus on the goniometer head of a Bruker D8 Venture Kappa DUO diffractometer equipped with Bruker Photon 100 CMOS detector. A suitable crystal of $[(C_6H_{11}NC)_2Au](AsF_6)_{0.50}(SbF_6)_{0.50}$ was mounted in the 90 K nitrogen cold stream provided by a Cryo Industries low-temperature apparatus on the goniometer head of a Bruker APEX II sealed-tube diffractometer and a charge-coupled device (CCD) detector. All data were collected with the use of MoKα (λ = 0.71073 Å) radiation. A multiscan absorption correction was applied with the program SADABS.[42] The structure was solved by a dual-space method (SHELXT)[43] and refined by full-matrix least-squares on F^2 (SHELXL-2017).[44]

Physical Measurements. IR spectra were recorded on a Bruker Alpha FT-IR spectrometer using attenuated total reflectance (ATR). Fluorescence excitation and emission spectra were recorded on a Perkin Elmer LS50B luminescence spectrophotometer. ESI-MS was conducted using an Agilent Technologies 1260 Infinity II apparatus coupled to an Agilent Technologies InfinityLab LC/MSD.

■ ASSOCIATED CONTENT

Supporting Information

The Supporting Information is available free of charge at https://pubs.acs.org/doi/10.1021/jacs.9b13168.

Figure SI-1. Comparison of X-ray powder diffraction data for: yellow $[(C_6H_{11}NC)_2Au^I](PF_6)$, yellow $[(C_6H_{11}NC)_2Au^I](PF_6)_{0.50}(SbF_6)_{0.50}$, and yellow $[(C_6H_{11}NC)_2Au^I](SbF_6)$ at 298 K. Figure SI-2. Photographs of a sample of $[(C_6H_{11}NC)_2Au^I](PF_6)_{0.50}(SbF_6)_{0.50}$ (PDF)

X-ray crystallographic file for $[(C_6H_{11}NC)_2Au](PF_6)_{0.50}(SbF_6)_{0.50}$ (CIF)

X-ray crystallographic file for $[(C_6H_{11}NC)_2Au](AsF_6)_{0.50}(SbF_6)_{0.50}$ (CIF)

X-ray crystallographic file for $[(C_6H_{11}NC)_2Au](PF_6)_{0.75}(AsF_6)_{0.25}$ (CIF)

https://dx.doi.org/10.1021/jacs.9b13168
J. Am. Chem. Soc. 2020, 142, 5689−5701

X-ray crystallographic file for $[(C_6H_{11}NC)_2Au](PF_6)_{0.75}(AsF_6)_{0.25}$ (CIF)
X-ray crystallographic file for $[(C_6H_{11}NC)_2Au](PF_6)_{0.75}(AsF_6)_{0.25}$ (CIF)
X-ray crystallographic file for $[(C_6H_{11}NC)_2Au](PF_6)_{0.25}(AsF_6)_{0.75}$ (CIF)
X-ray crystallographic file for $[(C_6H_{11}NC)_2Au](PF_6)_{0.50}(AsF_6)_{0.50}$ (CIF)
X-ray crystallographic file for $[(C_6H_{11}NC)_2Au](SbF_6)$ (CIF)
X-ray crystallographic file for $[(C_6H_{11}NC)_2Au](PF_6)_{0.50}(AsF_6)_{0.50}$ (CIF)
X-ray crystallographic file for $[(C_6H_{11}NC)_2Au](PF_6)_{0.25}(AsF_6)_{0.75}$ (CIF)
Video showing the thermochromic change, under UV irradiation, of a colorless, blue-luminescent crystal of $[(C_6H_{11}NC)_2Au](PF_6)_{0.50}(AsF_6)_{0.50}$ to its yellow, green-luminescent solid form (MOV)
Video showing the thermochromic change and melting of a colorless, blue-luminescent crystal of $[(C_6H_{11}NC)_2Au](PF_6)_{0.50}(AsF_6)_{0.50}$ (MOV)
Supplementary video captions (PDF)

AUTHOR INFORMATION

Corresponding Author

Alan L. Balch − *Department of Chemistry, University of California, Davis, Davis, California 95616, United States;* orcid.org/0000-0002-8813-6281; Email: albalch@ucdavis.edu

Authors

Lucy M. C. Luong − *Department of Chemistry, University of California, Davis, Davis, California 95616, United States*
Mark A. Malwitz − *Department of Chemistry, University of California, Davis, Davis, California 95616, United States*
Venoos Moshayedi − *Department of Chemistry, University of California, Davis, Davis, California 95616, United States*
Marilyn M. Olmstead − *Department of Chemistry, University of California, Davis, Davis, California 95616, United States;* orcid.org/0000-0002-6160-1622

Complete contact information is available at: https://pubs.acs.org/10.1021/jacs.9b13168

Notes

The authors declare no competing financial interest.

ACKNOWLEDGMENTS

We acknowledge the ARCS Foundation for two awards to L. M. C. Luong, the National Science Foundation (grant CHE-1807637) for partial support of this project, grant CHE-1531193 for the dual-source X-ray diffractometer, Prof. S. M. Kauzlarich and C. J. Perez for assistance with the powder diffraction data, Dr. M. J. Stevenson and Prof. M. C. Heffern for assistance with the mass spectrometry, and Dr. J. C. Fettinger for crystallographic help.

REFERENCES

(1) Wang, X.-D.; Wolfbeis, O. S.; Meier, R. J. Luminescent probes and sensors for temperature. *Chem. Soc. Rev.* **2013**, *42*, 7834−7869.
(2) Li, B.; Fan, H.-T.; Zang, S.-Q.; Li, H. Y.; Wang, L.-Y. Metal-containing crystalline luminescent thermochromic materials. *Coord. Chem. Rev.* **2018**, *377*, 307−329.
(3) Perruchas, S.; Le Goff, X. F.; Maron, S.; Maurin, I.; Guillen, F.; Garcia, A.; Gacoin, T.; Boilot, J.-P. Mechanochromic and Thermochromic Luminescence of a Copper Iodide Cluster. *J. Am. Chem. Soc.* **2010**, *132*, 10967−10969.
(4) Kato, M.; Ito, H.; Hasegawa, M.; Ishii, K. Soft Crystals: Flexible Response Systems with High Structural Order. *Chem. - Eur. J.* **2019**, *25*, 5105−5112.
(5) Balch, A. L. Dynamic Crystals: Visually Detected Mechanochemical Changes in the Luminescence of Gold and Other Transition-Metal Complexes. *Angew. Chem., Int. Ed.* **2009**, *48*, 2641−2644.
(6) Walters, D. T.; Aghakhanpour, R. B.; Powers, X. B.; Ghiassi, K. B.; Olmstead, M. M.; Balch, A. L. Utilization of a Nonemissive Triphosphine Ligand to Construct a Luminescent Gold(I)-Box That Undergoes Mechanochromic Collapse into a Helical Complex. *J. Am. Chem. Soc.* **2018**, *140*, 7533−7542.
(7) Seki, T.; Takamatsu, Y.; Ito, H. A Screening Approach for the Discovery of Mechanochromic Gold(I) Isocyanide Complexes with Crystal-to-Crystal Phase Transitions. *J. Am. Chem. Soc.* **2016**, *138*, 6252−6260.
(8) Seki, T.; Sakurada, K.; Muromoto, M.; Ito, H. Photoinduced single-crystal-to-single-crystal phase transition and photosalient effect of a gold(I) isocyanide complex with shortening of intermolecular aurophilic bonds. *Chem. Sci.* **2015**, *6*, 1491−1497.
(9) Wenger, O. S. Vapochromism in Organometallic and Coordination Complexes: Chemical Sensors for Volatile Organic Compounds. *Chem. Rev.* **2013**, *113*, 3686−3733.
(10) Zhang, X.; Li, B.; Chen, Z.-H.; Chen, Z.-N. Luminescence vapochromism in solid materials based on metal complexes for detection of volatile organic compounds (VOCs). *J. Mater. Chem.* **2012**, *22*, 11427−11441.
(11) Li, S.-Y.; Niklasson, G. A.; Granqvist, C. G. Thermochromic fenestration with VO_2-based materials: Three challenges and how they can be met. *Thin Solid Films* **2012**, *520*, 3823−3828.
(12) Zhang, X.; Li, B.; Chen, Z.-H.; Chen, Z.-N. Luminescence vapochromism in solid materials based on metal complexes for detection of volatile organic compounds (VOCs). *J. Mater. Chem.* **2012**, *22*, 11427−11441.
(13) Kunugi, Y.; Mann, K. R.; Miller, L. L.; Exstrom, C. L. A Vapochromic LED. *J. Am. Chem. Soc.* **1998**, *120*, 589−590.
(14) Buss, C. E.; Anderson, C. E.; Pomije, M. K.; Lutz, C. M.; Britton, D.; Mann, K. R. Structural Investigations of Vapochromic Behavior. X-ray Single-Crystal and Powder Diffraction Studies of $[Pt(CN\text{-}iso\text{-}C_3H_7)_4][M(CN)_4]$ for M = Pt or Pd. *J. Am. Chem. Soc.* **1998**, *120*, 7783−7790.
(15) Buss, C. E.; Mann, K. R. Synthesis and Characterization of Pt(CN-*p*-(C2H5)C6H4)2$(CN)_2$, a Crystalline Crystalline Vapoluminescent Compound That Detects Vapor-Phase Aromatic Hydrocarbons. *J. Am. Chem. Soc.* **2002**, *124*, 1031−1039.
(16) Grove, L. J.; Rennekamp, J. M.; Jude, H.; Connick, W. B. A New Class of Platinum(II) Vapochromic Salts. *J. Am. Chem. Soc.* **2004**, *126*, 1594−1595.
(17) Fernández, E. J.; López-de-Luzuriaga, J. M.; Monge, M.; Olmos, M. E.; Pérez, J.; Laguna, A.; Mohamed, A. A.; Fackler, J. P., Jr. $\{Tl[Au(C_6Cl_5)_2]\}_n$: A Vapochromic Complex. *J. Am. Chem. Soc.* **2003**, *125*, 2022−2023.
(18) Fernández, E. J.; López-de-Luzuriaga, J. M.; Monge, M.; Montiel, M.; Olmos, M. E.; Pérez, J.; Laguna, A.; Mendizabal, F.; Mohamed, A. A.; Fackler, J. P., Jr. A Detailed Study of the Vapochromic Behavior of $\{Tl[Au(C_6Cl_5)_2]\}_n$. *Inorg. Chem.* **2004**, *43*, 3573−3581.
(19) Albrecht, M.; Lutz, M.; Spek, A. L.; van Koten, G. Organoplatinum crystals for gas-triggered switches. *Nature* **2000**, *406*, 970−974.
(20) Bernstein, J. *Polymorphism in Molecular Crystals*; Oxford University Press: New York, 2008.
(21) Balch, A. L. Remarkable Luminescence Behaviors and Structural Variations of Two-Coordinate Gold(I) Complexes. *Struct. Bonding (Berlin, Ger.)* **2007**, *123*, 1−40.

(22) Yam, V. W.-W.; Au, V. K.-A.; Leung, S. Y.-L. Light-Emitting Self-Assembled Materials Based on d^8 and d^{10} Transition Metal Complexes. *Chem. Rev.* **2015**, *115*, 7589−7728.
(23) Schmidbaur, H.; Schier, A. Aurophilic interactions as a subject of current research: an up-date. *Chem. Soc. Rev.* **2012**, *41*, 370−412.
(24) Pyykkö, P. Theoretical chemistry of gold. III. *Chem. Soc. Rev.* **2008**, *37*, 1967−1997.
(25) Gussenhoven, E. M.; Fettinger, J. C.; Pham, D. M.; Malwitz, M. A.; Balch, A. L. A Reversible Polymorphic Phase Change which Affects the Luminescence and Aurophilic Interactions in the Gold(I) Cluster Complex, $[m_3\text{-}S(AuCNC_7H_{13})_3](SbF_6)$. *J. Am. Chem. Soc.* **2005**, *127*, 10838−10839.
(26) Ghimire, M. M.; Nesterov, V. N.; Omary, M. A. Remarkable Aurophilicity and Photoluminescence Thermochromism in a Homoleptic Cyclic Trinuclear Gold(I) Imidazolate Complex. *Inorg. Chem.* **2017**, *56*, 12086−12089.
(27) Ito, H.; Muromoto, M.; Kurenuma, S.; Ishizaka, S.; Kitamura, N.; Sato, H.; Seki, T. Mechanical stimulation and solid seeding trigger single-crystal-to-single-crystal molecular domino transformations. *Nat. Commun.* **2013**, *4*, 2009.
(28) Seki, T.; Sakurada, K.; Muromoto, M.; Seki, S.; Ito, H. Detailed Investigation of the Structural, Thermal, and Electronic Properties of Gold Isocyanide Complexes with Mechano-Triggered Single-Crystal-to-Single-Crystal Phase Transitions. *Chem. - Eur. J.* **2016**, *22*, 1968−1978.
(29) Liu, Q.; Xie, M.; Chang, X.; Gao, Q.; Chen, Y.; Lu, W. Correlating thermochromic and mechanochromic phosphorescence with polymorphs of a complex gold(I) double salt with infinite aurophilicity. *Chem. Commun.* **2018**, *54*, 12844−12847.
(30) White-Morris, R. L.; Olmstead, M. M.; Balch, A. L. Aurophilic Interactions in Cationic Gold Complexes with Two Isocyanide Ligands. Polymorphic Yellow and Colorless Forms of $[(Cyclohexyl\ Isocyanide)_2Au^I](PF_6)$ with Distinct Luminescence. *J. Am. Chem. Soc.* **2003**, *125*, 1033−1040.
(31) Malwitz, M. A.; Lim, S. H.; White-Morris, R. L.; Pham, D. M.; Olmstead, M. M.; Balch, A. L. Crystallization and Interconversions of Vapor-Sensitive, Luminescent Polymorphs of $[(C_6H_{11}NC)_2Au^I]^+(AsF_6)$ and $[(C_6H_{11}NC)_2Au^I](PF_6)$. *J. Am. Chem. Soc.* **2012**, *134*, 10885−10893.
(32) Krossing, I.; Raabe, I. Noncoordinating Anions—Fact or Fiction? A Survey of Likely Candidates. *Angew. Chem., Int. Ed.* **2004**, *43*, 2066−2090.
(33) Strauss, S. H. The Search for Larger and More Weakly Coordinating Anions. *Chem. Rev.* **1993**, *93*, 927−942.
(34) White-Morris, R. L.; Olmstead, M. M.; Jiang, F.; Tinti, D. S.; Balch, A. L. Remarkable Variations in the Luminescence of Frozen Solutions of $[Au\{C(NHMe)_2\}_2](PF_6)\cdot 0.5(Acetone)$. Structural and Spectroscopic Studies of the Effects of Anions and Solvents on Gold(I) Carbene Complexes. *J. Am. Chem. Soc.* **2002**, *124*, 2327−2336.
(35) Rios, D.; Pham, D. M.; Fettinger, J. C.; Olmstead, M. M.; Balch, A. L. Blue or Green Glowing Crystals of the Cation $[Au\{C(NHMe)_2\}_2]^+$. Structural Effects of Anions, Hydrogen Bonding, and Solvate Molecules on the Luminescence of a Two-Coordinate Gold (I) Carbene Complex. *Inorg. Chem.* **2008**, *47*, 3442−3451.
(36) Rios, D.; Olmstead, M. M.; Balch, A. L. Colorless, non-luminescent; colorless, luminescent; and yellow, luminescent crystals of the cation $[Au\{C(NHCH_3)(NHCH_2CH_2OH)\}_2]^+$. The roles of anions and hydrogen bonding in determining the aggregation of two-coordinate gold (I) cations. *Dalton Trans.* **2008**, 4157−4164.
(37) Saitoh, M.; Balch, A. L.; Yuasa, J.; Kawai, T. Effects of Counter Anions on Intense Photoluminescence of 1-D Chain Gold(I) Complexes. *Inorg. Chem.* **2010**, *49*, 7129−7134.
(38) MacDonald, J. C.; Dorrestein, P. C.; Pilley, M. M.; Foote, M. M.; Lundburg, J. L.; Henning, R. W.; Schultz, A. J.; Manson, J. L. Design of Layered Crystalline Materials Using Coordination Chemistry and Hydrogen Bonds. *J. Am. Chem. Soc.* **2000**, *122*, 11692−11702.
(39) Bouzaid, J.; Schultz, M.; Lao, Z.; Bartley, J.; Bostrom, T.; McMurtrie, J. Supramolecular Selection in Molecular Alloys. *Cryst. Growth Des.* **2012**, *12*, 3906−3916.
(40) Bouzaid, J.; Schultz, M.; Lao, Z.; Bostrom, T.; McMurtrie, J. Influences of Molecular Structure on Supramolecular Selection during Cocrystallization of Polypyridyl Metal Complexes. *Cryst. Growth Des.* **2015**, *15*, 62−69.
(41) Bruce, M. I.; Nicholson, B. K.; Shawkataly, O. B.; Shapley, J. R.; Henly, T. Synthesis of Gold-Containing Mixed-Metal Cluster Complexes. *Inorg. Syn.* **1989**, *26*, 324−328.
(42) Krause, L.; Herbst-Irmer, R.; Sheldrick, G. M.; Stalke, D. Comparison of silver and molybdenum microfocus X-ray sources for single-crystal structure determination. *J. Appl. Crystallogr.* **2015**, *48*, 3−10.
(43) Sheldrick, G. M. SHELXT - Integrated space-group and crystal-structure determination. *Acta Crystallogr., Sect. A: Found. Adv.* **2015**, *71*, 3−8.
(44) Sheldrick, G. M. *SHELXL*, Crystal structure refinement with SHELXL. *Acta Crystallogr., Sect. C: Struct. Chem.* **2015**, *71*, 3−8.

https://dx.doi.org/10.1021/jacs.9b13168
J. Am. Chem. Soc. 2020, 142, 5689−5701